Evaluating BIPV modules with respect to textural appearance, glare, colour and electricity yield

Helen Rose Wilson[1], Bruno Bueno[1], Johannes Eisenlohr[1], Tilmann E. Kuhn[1]
[1]Fraunhofer Institute for Solar Energy Systems ISE,
Heidenhofstr. 2,
79110 Freiburg, Germany
helen.rose.wilson@ise.fraunhofer.de, tel. +49 761 4588 5149

Key words: Building-integrated photovoltaics (BIPV), outdoor glare, bi-directional scattering distribution function (BSDF), ray-tracing, colour, electricity yield prediction

1. Abstract

BIPV modules are often visible as part of a façade or a roof, so it is important to know, not only how much electricity they will generate, but also how they will appear to an observer or interact with incident light. This paper thus addresses methods to evaluate module appearance (colour and surface gloss or mattness) and external glare from modules. It also discusses prediction of the electricity yield, since this is the primary task for every PV and BIPV installation and should always be taken into account, when BIPV systems are evaluated. For each property evaluated, not only the methodology but also some results obtained by applying it to different types of (BI)PV modules are presented. Each methodology is based on the measurement of module properties; in the case of glare and electricity yield prediction, system aspects of a BIPV installation and its surroundings are also presented in this paper.

2. Introduction

Building-integrated photovoltaics (BIPV) modules on roofs and facades are of great relevance for the energy transition, because they take advantage of extensive areas exposed to the sun that otherwise might not be available. In order to ensure broad acceptance of BIPV systems in society, methods for the evaluation of their visual and energy impact are needed.

3. Evaluation of appearance

The appearance of BIPV modules (e.g. degree of gloss, colour) depends on the position and direction of the observer, on the component's optical properties as well as on the lighting conditions by the sky (i.e. light intensity, spectrum and polarization from different regions of the sky dome).
Many widely used, state-of-the-art visualization tools are not yet able to accurately reproduce the appearance of innovative building materials. Most common renderers (e.g. V-Ray, Arnold, and Keyshot) do not support accurate spectral simulations. Others (e.g. Maxwell) implement spectral sky models but do not have angle-dependent material

models. Figure 1 shows a rendering with V-Ray of a stela at Fraunhofer ISE's headquarters, where different MorphoColor® PV modules are exposed.

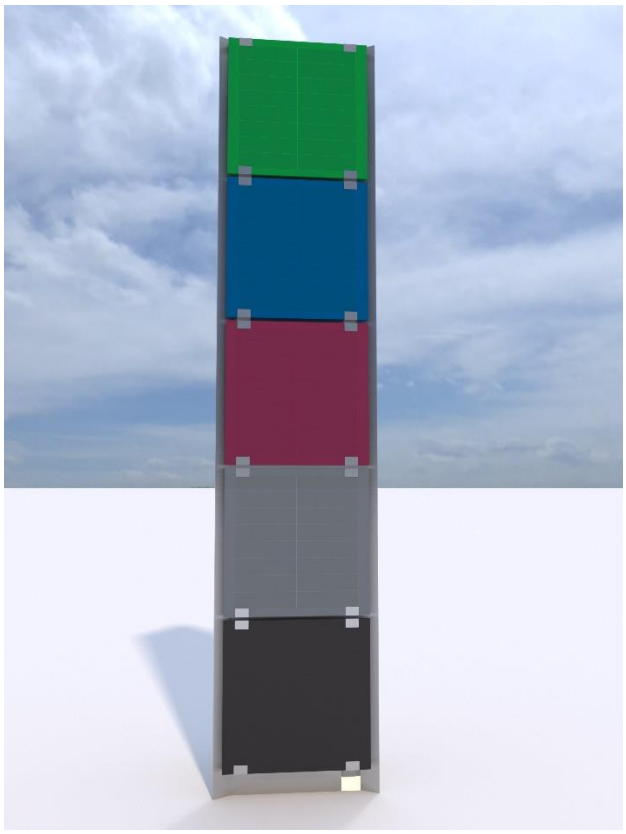

Figure 1: Rendering of a stela with different MorphoColor® PV modules at Fraunhofer ISE's headquarters with V-Ray (https://www.chaosgroup.com/3d-rendering-software). Spectral sky models and angle-dependent, spectral material models are not directly supported by V-Ray.

In large construction projects, it is common practice to use mock-ups to analyse the appearance of building facades. This is an expensive process, which could be replaced by efficient visualization tools. These tools, however, must be extended in order to capture the optical features of innovative BIPV components. In particular, they must account for the spectral, angular and polarization-dependent behaviour of building materials and for spectral, polarization-dependent sky models.

3.1. Angle-dependent optical properties of BIPV modules

The evaluation of textural appearance needs a method to distinguish between light that is reflected directly (or specularly), as from a glossy surface, or diffusely, as from a matt surface (Figure 2).

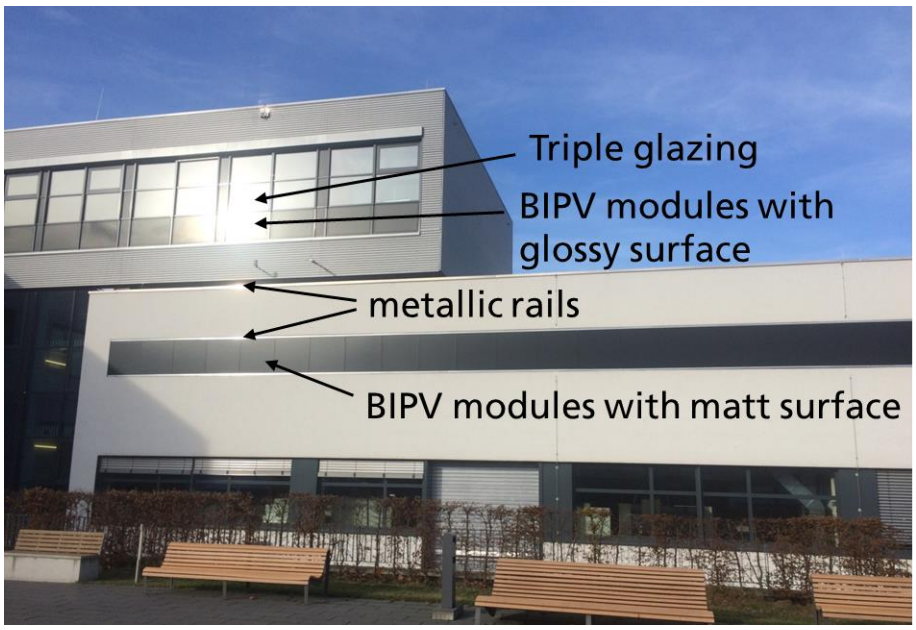

Figure 2: Examples of different types of BIPV modules with glossy and matt surfaces. Source: Fraunhofer ISE.

The distinction between direct and diffuse reflection is illustrated schematically in Figure 3. An integrating sphere featuring an aperture that can either be closed or allow directly reflected light to exit from the sphere is the optical device that is most commonly applied to make this distinction. The most widespread integrating spheres allow illumination at only near-normal incidence, but more advanced integrating spheres also allow measurements with illumination at oblique angles of incidence. By applying sophisticated ray-tracing simulation tools such as Radiance [1, also www.radiance-online.org], the textural appearance of either highly glossy or extremely matt BIPV modules can already be rendered convincingly on the basis of this binary distinction between direct and diffuse reflectance values.

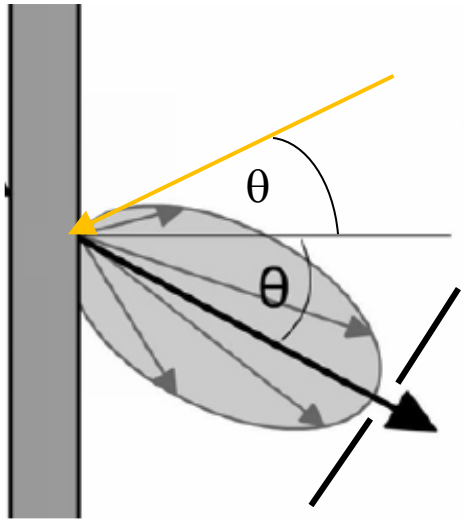

Figure 3: Different types of reflection from a surface. Yellow arrow: Light beam with an incidence angle θ. Black arrow: Directly reflected, quasi-parallel light at the emergent angle θ. Grey arrows: diffusely reflected light. Adapted from [2, Fig. 3].

However, the glass covers used on many PV modules are neither purely glossy nor purely matt, meaning that their reflection behaviour cannot be modelled adequately by applying either Fresnel equations or assuming Lambertian reflection. For (BI)PV modules with mixed modes of reflection, a BRDF (bidirectional reflectance distribution function) presents a suitable way to characterise the angle-dependent reflection behaviour of the surface. A BRDF quantifies the angular distribution of light that is reflected by a surface as a function depending on angles of both incidence and emergence [3]. BRDF images such as those in Figure 4 give a visual impression of the angular distribution of the light reflected by different PV samples for a specific incidence angle. The logarithmic colour scale corresponds to the signal intensity at a given angular position of the detector; the radial and azimuthal values in the two-dimensional, circular coordinate system characterise the polar angle θ and azimuth φ of the angular detector position in the three-dimensional, spherical coordinate system. Visual representations of the BRDF already allow “glossy” surfaces, with high BRDF values concentrated over a small angular region (Figure 4, left), to be distinguished from matter surfaces, with BRDF values that span a smaller range but are non-negligible over a larger angular region (Figure 4, right). By using the BRDF as input data to ray-tracing simulation tools, convincing images can be rendered also to convey the textural appearance of BIPV module surfaces that feature a mixture of specular and diffuse reflection. This applies particularly to the surfaces of PV modules that have been treated to reduce the risk of glare, by scattering the reflected light without affecting the energy efficiency of the module.

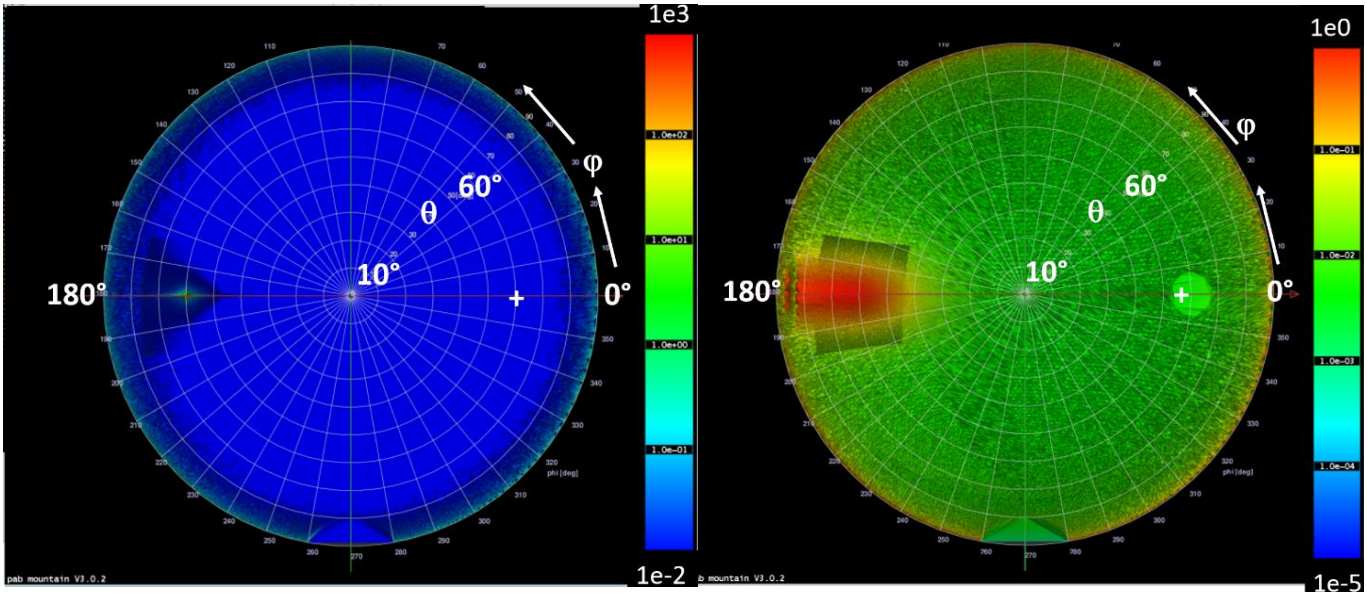

Figure 4: BRDF “top view” images of PV modules with specular reflection (left) and diffuse reflection (right) for radiation incident at theta_in = 60° and phi_in = 0°. The angular position of the incident light is marked with a white cross (+). Source: Fraunhofer ISE; reproduction authorized by NICE Solar Energy GmbH.

A three-dimensionally scanning photogoniometer pgII from pab Advanced Technologies Ltd. is used at Fraunhofer ISE to measure BRDFs (Figure 5)[4]. The instrument is equipped with halogen and xenon lamps as light sources and a variety of detectors, including a filtered silicon diode with a V(λ) spectral response for broadband light measurements, a broadband silicon diode, a broadband InGaAs diode and diode array spectrometers for the visible and NIR spectral ranges. By rotating the centrally, vertically mounted sample around horizontal and vertical axes (Figure 5), any combination of incident altitude and azimuth angles can be selected. The outgoing rays are measured with fine angular resolution by scanning the detector over the surface of a virtual sphere centred on the intersection of the two rotational axes for the sample (Figure 6). BRDFs are measured over the surface of the “reflection hemisphere” that is located between the light source and the sample plane. The analogous function for transmission, the BTDF, is measured over the “transmission hemisphere” that is located on the opposite side of the sample to the light source.

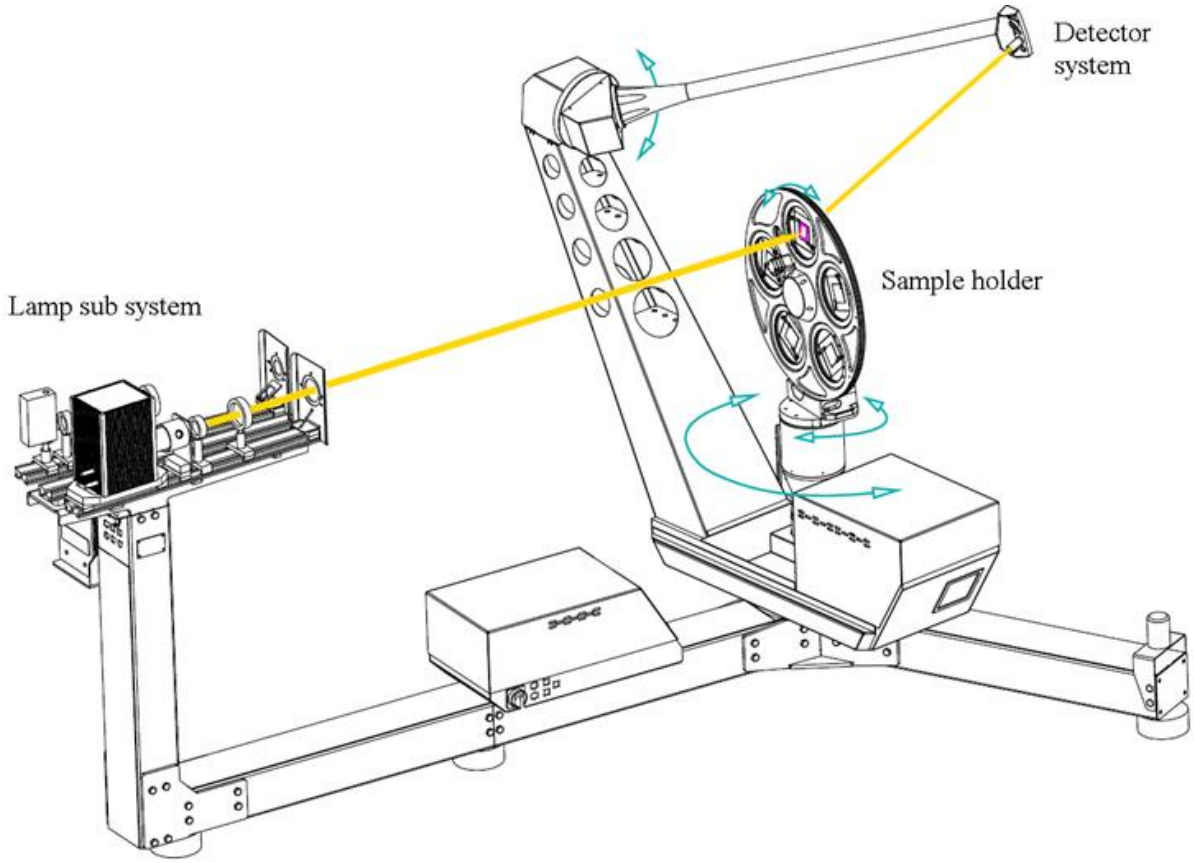

Figure 5: Isometric view of the photogoniometer pgII at Fraunhofer ISE, showing the light source, the detector head and the the phirot5 sample holder for five different samples, and indicating the planes of rotation for the sample holder and the detector arms. Source: Peter Apian-Bennewitz, pab advanced technologies Ltd.

Figure 6: Time-exposure image of the three-dimensionally scanning photogoniometer pgII at Fraunhofer ISE, indicating the virtual sphere surface traced out by the detector. For measurements, the detector paths are much more closely spaced and can be programmed to characterise sharp peaks in light intensity with very fine angular resolution. Source: Fraunhofer ISE.

Direct-hemispherical transmittance or reflectance values can be calculated by integration of the BTDF or BRDF values over the surface of the entire transmission or reflection hemisphere, respectively. Direct-direct transmittance or reflectance values are calculated by integrating the BTDF or BRDF values over only a small segment of the surface that is centred on the emergent angle of interest.

3.2. Spectrally dependent optical properties of BIPV modules

Broadband measurements of light, e.g. using a filtered V(λ) detector that corresponds to the spectral sensitivity of the light-adapted human eye, are suitable for assessing textural appearance and glare. However, finer spectral resolution is needed for evaluation of colour. Figure 7 shows the different colours of visible light and the wavelengths to which they correspond within a solar spectrum.

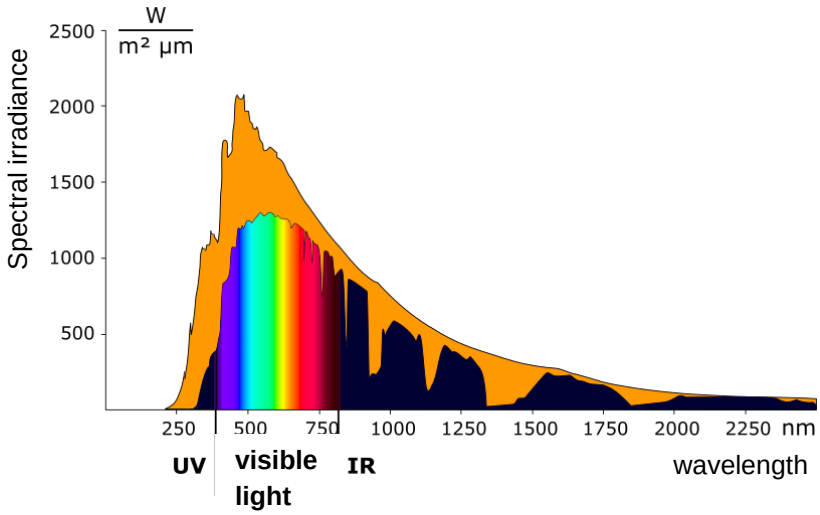

Figure 7: Representation of solar spectrum including colours of visible light. Source: Wikipedia Commons

Again, measurement instruments with different degrees of sophistication are available for the task, ranging from hand-held colorimeters, through laboratory-grade spectrophotometers equipped with integrating spheres and goniometric photometers equipped with RGB detectors, to goniometric spectrophotometers that provide both spatially and spectrally resolved data on reflectance properties. The method of choice depends on the level of colour information needed, e.g. coarse colour classification at the early architectural design phase or evaluation of colour constancy of BIPV modules for different viewing angles.

As an example, Figure 8 shows the direct-hemispherical reflectance spectra of a green MorphoColor® PV module, which were measured at Fraunhofer ISE using an integrating sphere accessory to a commercial laboratory-grade spectrophotometer. From this, the calculated coloured appearance of the same MorphoColor® PV module when illuminated by light different incidence angles is depicted in Figure 9.

Once the spectral reflectance data is available, it can be weighted to obtain colour coordinates in different colour spaces, as defined in [5]. Figure 10 shows a representation of the so-called L*a*b* colour space, in which equal perceived colour differences correspond to equal Euclidean distances. This provides a convenient metric for evaluating colour constancy.

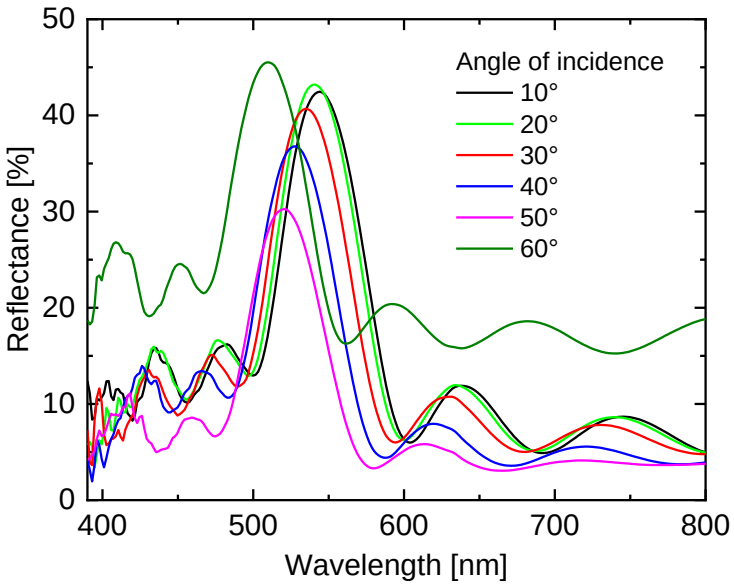

Figure 8: Direct-hemispherical reflectance spectra of a green MorphoColor® PV module for different incidence angles of the incoming light. Source: [6]

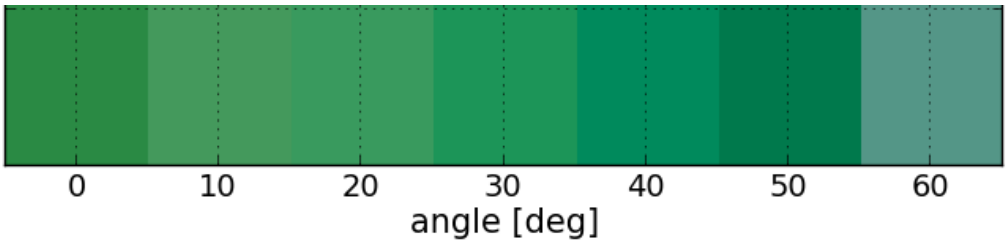

Figure 9: Visual impression of a green MorphoColor® PV module as calculated from the spectra of Figure 8 for different incidence angles of the incoming light. Source: [6]

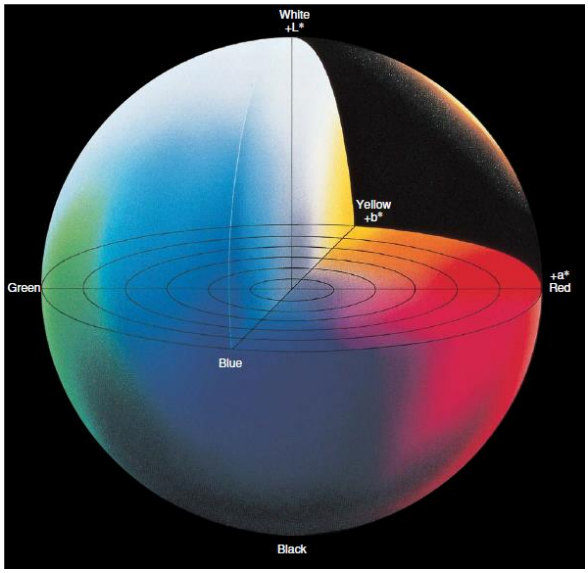

*Figure 10: Representation of colour solid for L*a*b* colour space. Source: [7, Fig. 8]; reproduction authorized by Konica Minolta Sensing Europe B.V.*

4. Evaluation of glare

Measurement-based determination of the BRDF is crucial for accurate glare evaluation and correct evaluation of glare-reduction measures. The risk of outdoor glare due to reflections from the PV modules is sometimes cited as an argument against the installation of BIPV systems, although the risk of glare for specularly reflecting glass covers on PV modules is comparable to or lower than for conventional glazing units. However, as some authorization procedures in Germany are different for electricity-generating systems than for building products, uncertainty about outdoor glare may lead to legal conflicts with unpredictable outcomes that delay BIPV projects. The lack of a uniform and universally recognised quantitative evaluation method means that the interpretation of legal requirements is unclear and leads to individual and even contradictory results. Several different glare metrics are applied for different purposes (e.g. road traffic, pedestrians, aviation, etc.). These metrics, based on radiometric or photometric quantities and thresholds, are generally derived from simplified theoretical assumptions (e.g. always cloudless skies, maximum direct normal irradiance, average integrated reflectance of PV) that do not readily translate to subjective glare perception. There is thus an urgent need for a methodology, which can already be applied during the planning phase, to quantify and analyse the magnitude of glare that could arise. Based on this methodology, PV modules with different surface treatments that reduce the risk of glare (e.g. as characterized in Figure 4, right-hand image) can be compared objectively and the most suitable type for a given application and location can be selected.

The methodology that we propose for glare evaluation is based on a combination of BRDF measurements of PV modules in the laboratory and ray-tracing to determine how much sunlight (and skylight) is reflected and where it would be perceived, when the modules are installed at a specific location and orientation. To evaluate the glare caused by an installation of PV modules with optical properties corresponding to the BRDF determined for the samples, initially the geometrical configuration of the (BI)PV array of modules is modelled. For the incident light, well-established algorithms for the solar position and the light distribution over the sky hemisphere are applied. The analysis is based on luminance results that are simulated using the validated Radiance ray-tracing software, using information on the geometrical configuration of the (BI)PV installation and its surroundings, the incident illumination from the sun and the sky, and the BRDF of the modules. The bi-directional reflectance properties of the PV modules are represented by a Radiance material primitive called BSDF, which can take a tensor-tree BRDF as an input. The Radiance program provides the user with a suite of tools to convert raw BRDF data into a tensor-tree format, including BRDF data measured with a pgII photogoniometer as described above.

Luminance maps over the specified PV installation, as perceived by an observer at given viewing points, are used to evaluate the glare caused by PV modules of different types. This approach allows “bright spots” in the field of view to be identified. The luminance maps can be compared with reference luminance maps such as for a conventional building envelope surface. Alternatively, maximum values from the maps can be extracted

and compared to limits such as those specified by guidelines referring to the surroundings of airfields [8] or the urban environment [9, 10]. In this way, an objective glare guide is provided that allows PV modules with the most suitable type of front surface treatments to be chosen for a given building or installation site.

As an example, the use of BRDF data sets to evaluate the risk of glare is illustrated for the case of a ground-mounted PV array near an airfield. However, the same methodological approach can also be applied to BIPV installations, but using benchmark criteria that have been developed for the urban environment to rate the glare risk. Using the BRDF data sets of the modules characterised in Figure 4, the luminance images in Figure 11 were calculated for an observer located at a position intercepting sunlight that is specularly reflected by the module array, i.e. where the ray reflected by a flat, glossy surface is expected.

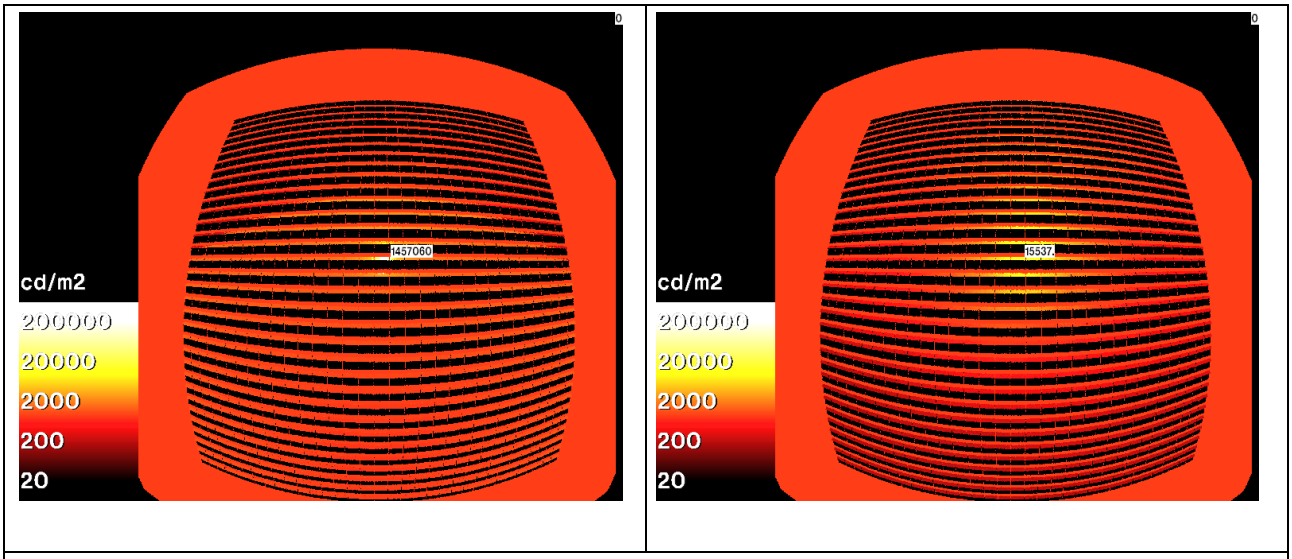

Figure 11: Luminance images of a ground-mounted array equipped with PV modules corresponding to those characterised in Figure 4 with direct reflection (left) and predominantly diffuse reflection (right). The images are for an observation point situated in the path of the specularly reflected sunlight. The maximum luminance value is labelled in each image. The same methodology can be applied to evaluate the glare risk objectively from a BIPV installation. Source: Fraunhofer ISE; reproduction authorized by NICE Solar Energy GmbH.

Comparing the maximum luminance value of each image, it is evident that the glossy left-hand module clearly exceeds the limit of 20,000 cd/m^2 specified by [8] with reference to the surroundings of airfields, whereas the right-hand type of module, with its diffuse reflectance, remains below the specified limit, for the illustrated combination of solar position, the observer's location and viewing direction, and the location and orientation of the PV array. For a given airfield at a specific location, with well-defined flight paths, analogous calculations can be made to check whether glare can be avoided by using modules with a suitable surface treatment in a (BI)PV installation, for **all** relevant combinations of illumination and observation points.

5. Evaluation of electricity yield

The optical properties can also have a strong influence on the performance of BIPV modules and complete systems. Whereas simplified models at the module level can be applied for free-standing or rooftop configurations, geometrically and electrically complex BIPV systems require tools that are fully flexible with regard to the geometrical and electrical design of the system and a description at the solar cell level. Detailed optical properties must also be taken into account. Fraunhofer ISE has developed a simulation tool suite that allows such a detailed description and yield optimization. It was developed in [11] and applied and presented e.g. in [12] and [13]. To address the main challenges of BIPV yield simulation (complex and individual module and system geometry, individual electrical string and interconnection schemes, partial shading etc.), the tool suite comprises five main steps: calculation of the time-dependent irradiance (1) and temperature (2) of each solar cell, determination of the IV characteristic of each solar cell in the system at every time step (3), calculation of the system's DC (4) and AC (5) yield. Figure 12 gives a brief overview of these steps and the most important required input data.

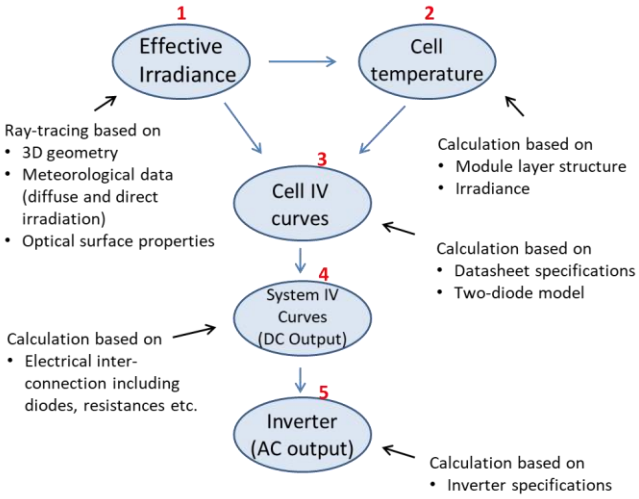

Figure 12: Schematic description of the five main steps for a detailed BIPV simulation. For each time step, the irradiance on each solar cell, the temperature of each solar cell, the cell IV characteristic for each temperature/irradiance combination, the system IV characteristic and the AC output are calculated.

In step (1), we use the Radiance ray-tracing tool [1]. The direct and diffuse irradiance on each solar cell for each time step is calculated by backward ray-tracing. A correction of the irradiance values according to the angle of incidence (IAM modifier) is introduced. This IAM modifier needs to be determined carefully, especially for advanced optical surface textures. In step (2), the cell temperature of each solar cell for each time step is calculated; different models are available for this [14]. It is important to consider the actual mounting situation, which for BIPV often leads to significantly higher temperatures than for well ventilated field installations. In step (3) the cell IV characteristics are calculated for all occurring combinations of irradiance and temperature. Usually, the two-diode model with parameters fitted based on data sheet parameters is used, as it allows for an accurate

description also under low-light behaviour, which is often the case in BIPV. Step (4) comprises the interconnection of all individual IV characteristics based on the chosen module, string and system layout. Also bypass diodes and further resistances (e.g. cabling) are taken into account. This step already requires some information about the operation of the system, which is usually controlled by the inverter. For example, the starting voltages or the maximum power point range of the inverter are considered. Alternatively, DC-DC power optimizers can be introduced in step (4), as is described in detail in [15]. Finally, in step (5), the DC-AC conversion efficiency and the final AC output is calculated based on data sheet specifications of the inverter. Usually, a parametric model of the inverter is used [16].
As an application example of this methodology, Figure 13 shows the south-facing BIPV façade of the Z3 building owned by Ed. Züblin AG in Stuttgart and the four different configurations for the module electric circuit that were modelled. As the BIPV modules are partially shaded by the wooden fins of the façade, an optimized electric circuit design was proposed that separates the module into three cell strings (left cell column, right cell column, three middle cell columns, (Figure 13C), that are connected independently of each other with the corresponding cell strings of the adjacent modules above and below. The yield simulation tool allows a “what-if” analysis, considering a simple configuration with all cells in series (Figure 13A) without bypass diodes, adding bypass diodes (B), the already described approach with 3 separate strings without (C) and with (D) bypass diodes. This results in the following DC electricity yield (the result of step (4) described above): Compared to the simple reference case with all cells within a module connected in series, adding bypass diodes at appropriate positions leads to an increase of the DC output power by 9 %, using three separate strings leads to an increase of 11 % and using three strings and diodes results in an increase of 13%.

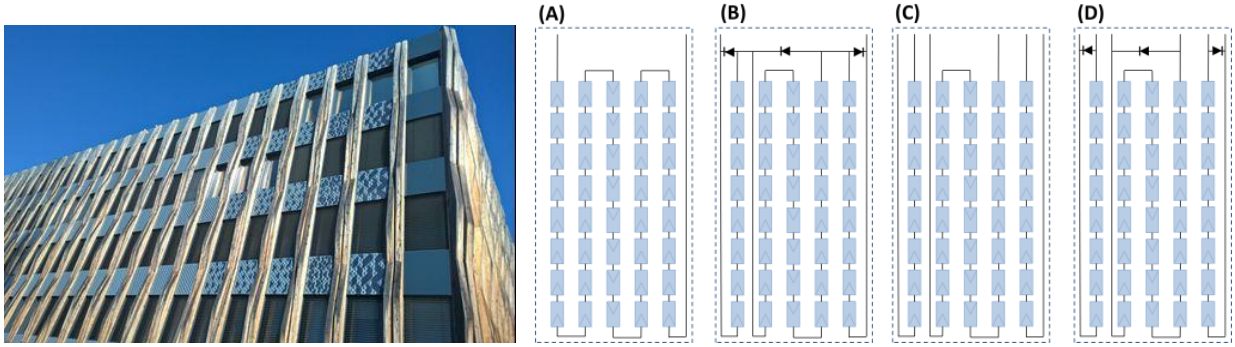

Figure 13: The BIPV façade of the Z3 building in Stuttgart. The PV panels are mounted in the rows between the windows and have different screen-printed patterns on their front glass covers. Source: Ed. Züblin AG. Four different electric module circuit configurations with two (A, B) or six (C,D) external connectors and without (A,C) or with (B,D) bypass diodes [6].

To demonstrate the detailed effect of adding bypass diodes or using separate strings, Figure 14 shows a typical diurnal profile for the DC output of the complete façade. The four different variations of Figure 13 can be clearly distinguished by different output levels in the morning and the afternoon/evening. At these times, the wooden fins cause shading of

the left or right cell columns within the modules due to the oblique incidence angle of the direct solar irradiation. Around noon, when the direct irradiation is incident from the south, no partial shading occurs and the bypass diodes and/or multiple strings have no effect.

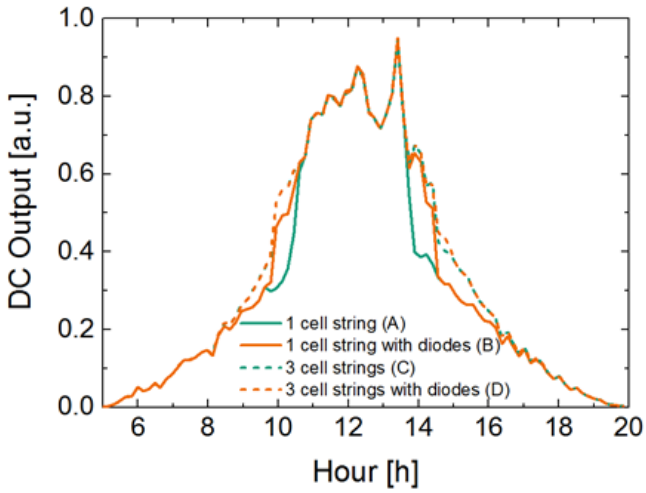

Figure 14: Simulated DC output of the complete BIPV system during one typical day. The four different curves correspond to the four different circuit designs from Figure 13. The influence of partial shading in the morning and afternoon is clearly visible and decreases from (A) to (D) [13].

6. Conclusions

Many different aspects should be considered when a BIPV system is being planned. The methods and results presented in this paper demonstrate that some evaluation methods are already available that are suitable to assess the textural appearance, colour, glare effect and electricity yield of BIPV modules at the component and system level. They allow the innovative features of products that extend beyond the start of the art, such as glare-reducing surface treatments, to be appropriately communicated. In this active field of research, further evaluation methods can be expected soon.

7. Acknowledgements

This study has partially received funding from the European Union's Horizon 2020 research and innovation programme under grant agreement No. 952886. The sole responsibility for the content of this study lies with the authors. It does not necessarily reflect the opinion of the European Community. The authors thank their colleagues at Fraunhofer ISE for input relating to the MorphoColor® modules. The permission granted by Peter Apian-Bennewitz of pab advanced technologies Ltd, and representatives of NICE Solar Energy GmbH, Ed. Züblin AG and Konica Minolta Sensing Europe B.V. to publish their illustrations is gratefully acknowledged.

8. References

1. G. Ward, *The RADIANCE lighting simulation and rendering system*, in Conf. Proc. Siggraph '94, vol. 28, pp. 459-472, 1994.
2. EN 14500:2020, *Blinds and Shutters – Thermal and visual comfort – test and calculation methods*, CEN
3. ASTM E 2387-05 (reapproved 2011), *Standard Practice for Goniometric Optical Scatter Measurements*
4. P. Apian-Bennewitz, *New scanning gonio-photometer for extended BRTF measurements*, SPIE Optics + Photonics 2010, San Diego, USA, paper 7792-24
5. CIE 015:2018, *Colorimetry*, CIE International Commission on Illumination, Colorimetry, Technical Report, 4th Edition, Commission Internationale de l´Eclairage, ISBN 978-3-902842-13-8, Vienna 2018
6. B. Bläsi, T. Kroyer, O. Höhn, M. Wiese, C. Ferrar, U. Eitner, T.E. Kuhn, *Morpho butterfly inspired coloured BIPV modules*, 33rd EU-PVSEC, Amsterdam, The Netherlands, 25 - 29.9. 2017
7. *Precise Color Communication*, downloaded from https://www.konicaminolta.com/instruments/knowledge/color/pdf/color_communication.pdf on 25.02.2020
8. EU Regulation No 139/2014, *Easy Access Rules for Aerodromes*
9. Bund-/Länder-Arbeitsgemeinschaft für Immissionsschutz (LAI), *Hinweise zur Messung, Beurteilung und Minderung von Lichtimmissionen*, downloaded on 3.3.2020 from https://www.lai-immissionsschutz.de/documents/lichthinweise-2015-11-03mit-formelkorrektur_aus_03_2018_1520588339.pdf
10. State of Brandenburg, *Leitlinie des Ministeriums für Umwelt, Gesundheit und Verbraucherschutz zur Messung und Beurteilung von Lichtimmissionen* (Licht-Leitlinie). Amtsblatt für Brandenburg - Nr. 21, 28-May-2014.
11. W. Sprenger, *Electricity yield simulation of complex BIPV systems* (Fraunhofer-Verlag, 2013).
12. W. Sprenger, H. R. Wilson, and T. E. Kuhn, *Electricity yield simulation for the building-integrated photovoltaic system installed in the main building roof of the Fraunhofer Institute for Solar Energy Systems ISE*, Solar Energy **135**, 633–643 (2016).
13. J. Eisenlohr, H.R. Wilson, T.E. Kuhn, *Detailed Modelling of Building-Integrated Photovoltaics - From Component and Environmental Data to the System Output*, 33rd European Photovoltaic Solar Energy Conference and Exhibition; 2118-2122. DOI: 10.4229/EUPVSEC20172017-6DO.11.1.
14. Y. B. Assoa, L. Mongibello, A. Carr, B. Kubicek, M. Machado, J. Merten, S. Misara, F. Roca, W. Sprenger, M. J. Wagner, S. Zamini, T. Baenas, and P. Malbranche, *Thermal analysis of a BIPV system by various modelling approaches*, Sol Energy **155**, 1289–1299 (2017).
15. J. Eisenlohr, S. Gasparotto, H. R. Wilson, T. E. Kuhn, *DC-DC Power Optimizers for Building-Integrated Photovoltaic Applications - A Simulation-Based Evaluation*,

(2018); 35th European Photovoltaic Solar Energy Conference and Exhibition; 1123-1126
16. H. Schmidt and D. U. Sauer, *Praxisgerechte Modellierung und Abschätzung von Wechselrichter-Wirkungsgraden*, Sonnenenergie **4**, 43–47 (1996).